J|A|C|S ARTICLES

Published on Web 07/15/2010

Pairing Fullerenes and Porphyrins: Supramolecular Wires That Exhibit Charge Transfer Activity

Florian Wessendorf,[†] Bruno Grimm,[‡] Dirk M. Guldi,[‡,*] and Andreas Hirsch*[,†]

Department of Chemistry and Pharmacy & Interdisciplinary Center for Molecular Materials (ICMM), Friedrich-Alexander-Universität Erlangen-Nürnberg, Henkestraβe 42, 91054 Erlangen, Germany and Egerlandstraβe 3, 91058 Erlangen, Germany

Received March 13, 2010; E-mail: andreas.hirsch@chemie.uni-erlangen.de; dirk.guldi@chemie.uni-erlangen.de

Abstract: A concept is elaborated of pairing electron donors and electron acceptors that share a common trait, wire-like features, as a powerful means to realize a new and versatile class of electron donor−acceptor nanohybrids. Important variables are fine-tuning (i) the complexation strength, (ii) the electron/energy transfer behavior, and (iii) the solubilities of the resulting architectures. In particular, a series of supramolecular porphyrin/fullerene hybrids assembled by the hydrogen bonding of Hamilton receptor/cyanuric acid motif has been realized. Putting the aforementioned variables into action, the association constants (K_{ass}), as they were determined from ^{1}H NMR and steady-state fluorescence assays, were successfully tweaked with values in the range of 10^4-10^5 M^{-1}. In fact, our detailed studies corroborate that the latter reveal a dependence on the nature of the spacer, that is, *p*-phenylene-ethynylene, *p*-phenylene-vinylene, *p*-ethynylene, and fluorene, as well as on the length of the spacer. Complementary performed transient absorption studies confirm that electron transfer is indeed the modus operandi in our novel class of electron donor−acceptor nanohybrids, while energy transfer plays, if any, only a minor role. The accordingly formed electron transfer products, that is, one-electron oxidized porphyrins and one-electron reduced fullerenes, are long-lived with lifetimes that reach well into the time domain of tens of nanoseconds. Finally, we have used the distance dependence on electron transfer, charge separation and charge recombination, to determine for the first time a β value (0.11 $Å^{-1}$) for hydrogen-bonding-mediated electron transfer.

Introduction

One of the most interesting challenges in the field of nanoscale electronics lies in the mediation of charges/electrons between mutually interacting components.[1] To this end, a combination of the rapidly evolving fields of nanostructured materials and supramolecular chemistry provides an attractive strategy for constructing large and complex, yet highly ordered, molecular and supramolecular entities, with specific functions.[2−13] Inspired by the natural photosynthetic apparatus, in which chlorophylls (i.e., bacteriochlorophyll dimer, cytochrome C) harvest and convert sunlight, cascades of short-range/multistep electron transfer events have been the subject of extensive studies.[2−4] Because of the rich photo- and redox chemistry of porphyrins and metalloporphyrins, they have been probed as integrative components in photosynthetic reaction center models.[8−10] Here, porphyrins/metalloporphyrins serve several functions ranging from harvesting light through most of the visible part of the solar spectrum to electron transfer and electron transport. Multifunctional fullerenes, on the other hand, are

[†] Friedrich-Alexander-Universität Erlangen-Nürnberg, Henkestraβe 42.
[‡] Friedrich-Alexander-Universität Erlangen-Nürnberg, Egerlandstraβe 3.

(1) Carroll, R. L.; Gorman, C. B. *Angew. Chem., Int. Ed.* **2002**, *41*, 4378–4400.
(2) Kirmaier, C.; Holton, D. In *The Photosynthetic Reaction Center*; Deisenhofer, J., Norris, J. R., Eds.; Academic Press: San Diego, CA, 1993; Vol. II, pp 49−70.
(3) (a) Remy, A.; Gerwert, K. *Nat. Struct. Biol.* **2003**, *10*, 637–644. (b) Okumura, M. Y.; Paddock, M. L.; Graige, M. S.; Feher, G. *Biochim. Biophys. Acta* **2000**, *1458*, 138–163.
(4) Boxer, S. G. *Annu. Rev. Biophys. Bioeng.* **1990**, *19*, 267.
(5) *The Reaction Center of Photosynthetic Bacteria*; Michel-Beyerle, M. E., Ed.; Springer: Berlin, 1996.
(6) (a) Fukuzumi, S.; Imahori, H. In *Electron Transfer in Chemistry*; Balzani, V., Ed.; Wiley-VCH: Weinheim, 2001; Vol. 2, pp 927−975. (b) Fukuzumi, S.; Guldi, D. M. In *Electron Transfer in Chemistry*; Balzani, V., Ed.; Wiley-VCH: Weinheim, 2001; Vol. 2, pp 270−337. (c) Fukuzumi, S. *Org. Biomol. Chem.* **2003**, *1*, 609–620.
(7) Guldi, D. M.; Kamat, P. V. In *Fullerenes, Chemistry, Physics, and Technology*; Kadish, K. M., Ruoff, R. S., Eds.; Wiley-Interscience: New York, 2000; pp 225−281.
(8) (a) Imahori, H.; Tamaki, K.; Yamada, H.; Yamada, K.; Sakata, Y.; Nishimura, Y.; Yamazaki, I.; Fujitsuka, M. O.; Ito, O. *Carbon* **2000**, *38*, 1599. (b) Fukuzumi, S.; Imahori, H.; Yamada, H.; El-Khouly, M. E.; Fujitsuka, M.; Ito, O.; Guldi, D. M. *J. Am. Chem. Soc.* **2001**, *123*, 2571–2575.
(9) Imahori, H.; Tamaki, K.; Guldi, D. M.; Luo, C.; Fujitsuka, M.; Ito, O.; Sakata, Y.; Fukuzumi, S. *J. Am. Chem. Soc.* **2001**, *123*, 2607–2617.
(10) Imahori, H.; Guldi, D. M.; Tamaki, K.; Yoshida, Y.; Luo, C.; Sakata, Y.; Fukuzumi, S. *J. Am. Chem. Soc.* **2001**, *123*, 6617–6628.
(11) (a) Imahori, H.; Hagiwara, K.; Akiyama, T.; Aoki, M.; Taniguchi, S.; Okada, T.; Shirakawa, M.; Sakata, Y. *Chem. Phys. Lett.* **1996**, *263*, 545–550. (b) Tkachenko, N. V.; Guenther, C.; Imahori, H.; Tamaki, K.; Sakata, Y.; Fukuzumi, S.; Lemmetyinen, H. *Chem. Phys. Lett.* **2000**, *326*, 344–350.
(12) Vehmanen, V.; Tkachenko, N. V.; Imahori, H.; Fukuzumi, S.; Lemmetyinen, H. *Spectrochim. Acta, Part A* **2001**, *57*, 2229–2244.
(13) (a) Imahori, H. *Org. Biomol. Chem.* **2004**, *2*, 1425–1433. (b) Imahori, H.; Yamada, H.; Guldi, D. M.; Endo, Y.; Shimomura, A.; Kundu, S.; Yamada, K.; Okada, T.; Sakata, Y.; Fukuzumi, S. *Angew. Chem., Int. Ed.* **2002**, *41*, 2344–2347. (c) Imahori, H.; Tamaki, K.; Araki, Y.; Sekiguchi, Y.; Ito, O.; Sakata, Y.; Fukuzumi, S. *J. Am. Chem. Soc.* **2002**, *124*, 5165–5174.

 10.1021/ja101937w

known for their unique electron-accepting features. In fact, these three-dimensional electron acceptors hold great promise on account of their small reorganization energies in electron transfer reactions and have exerted noteworthy impact on the improvement of light-induced charge-separation.[14] In short, porphyrins/metalloporphyrins and fullerenes are molecular architectures ideally suited for devising integrated, multicomponent model systems to transmit and process solar energy.[15−17] Photoexcitation of the porphyrin/metalloporphyrin by visible light is readily followed by an electron transfer to guarantee the formation of a radical ion pair state, that is, the one-electron oxidized radical cation and the one-electron reduced radical anion of the porphyrin and the fullerene, respectively.[8−13]

The most far-reaching observation is that charge-recombination in metalloporphyrin/fullerene couples is located deep in the "inverted region" of the Marcus parabola, regardless of linkage, distance, and orientation. By contrast, lowering the driving force via replacing the metalloporphyrins with the better electron donors ferrocene or tetrathiafulvalene, while keeping all other parameters (i.e., distance, acceptor, solvent, temperature, etc.) constant, shifts the dynamics into the normal region. This variation is of great advantage in determining parameters such as electronic coupling (V), reorganization energy (λ), and attenuation factor (β) with high accuracy.[18] These parameters have key character for material design considerations with the objective to prolong the lifetime of the energetic radical ion pair states, while, simultaneously, optimizing the efficiency of charge separation.

Up to now, most electron donor−acceptor systems are based on the use of covalent linkages. Hereby, the linkage mediates the distance, spatial orientation, and flexibility between the donor and acceptor components. Much less is, however, known about noncovalent linkages en-route toward electron donor−acceptor nanohybrids and the function of the intervening spacers.[17] In a recent example, we introduced electron donor−acceptor systems comprising noncovalent electrostatic interactions, where oppositely charged fullerenes and porphyrins/cytochrome C interact tightly with each other. Sufficiently strong electronic couplings powered an intrahybrid charge separation in these nanohybrids.[15] This approach turned out to be very promising for constructing photovoltaic devices with efficient solar energy conversion performances.[19]

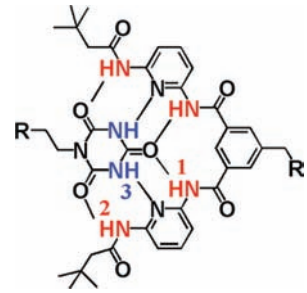

Figure 1. Schematic representation of the complementary hydrogen-bonding motif of a cyanuric acid derivative and a Hamilton receptor.

Nevertheless, the most compelling supramolecular motif is hydrogen bonding. Although hydrogen bonding bears great potential for the realization of highly directional self-assemblies, only a few examples of electron donor−acceptor nanohybrids, using porphyrins/metalloporphyrins and fullerenes, have been reported so far.[17,19] We have recently introduced the Hamilton-receptor/cyanuric acid binding motif (Figure 1)[20] to self-assemble porphyrins/metalloporphyrins together with fullerodendrimers[17a,b] as well as hydrogen-bonded complexes containing *N*,*N*-dimethylanilines, flavines,[21a] and supramolecular wires.[21b] Importantly, the six-point hydrogen-bonding motif leads to comparatively strong binding between hosts and guests with association constants K_{ass} that range in apolar solvents (i.e., dichloromethane and toluene) from 10^3 to 10^{12} M^{-1}.

(14) Guldi, D. M. *Chem. Soc. Rev.* **2002**, *31*, 22–36.
(15) (a) D'Souza, F.; Deviprasad, G. R.; El-Khouly, M. E.; Fujitsuka, M.; Ito, O. *J. Am. Chem. Soc.* **2001**, *123*, 5277–5284. (b) Regev, A.; Galili, T.; Levanon, H.; Schuster, D. I. *J. Phys. Chem. A* **2006**, *110*, 8593–8598. (c) Guldi, D. M.; Zilbermann, I.; Anderson, G.; Li, A.; Balbinot, D.; Jux, N.; Hatzimarinaki, M.; Hirsch, A.; Prato, M. *Chem. Commun.* **2004**, *6*, 726–727. (d) Balbinot, D.; Atalick, S.; Guldi, D. M.; Hatzimarinaki, M.; Hirsch, A.; Jux, N. *J. Phys. Chem. B* **2003**, *107*, 13273–13279. (e) Hartnagel, U.; Balbinot, D.; Jux, N.; Hirsch, A. *Org. Biomol. Chem.* **2006**, *4*, 1785–1795.
(16) (a) D'Souza, F.; El-Khouly, M. E.; Gadde, S.; Zandler, M. E.; McCarty, A. L.; Araki, Y.; Ito, O. *Tetrahedron* **2005**, *62*, 1967–1978. (b) Guldi, D. M. *Chem. Commun.* **2000**, *5*, 321–327. (c) Sessler, J. S.; Wang, B.; Springs, S. L.; Brown, C. T. In *Comprehensive Supramolecular Chemistry*; Atwood, J. L., Davies, J. E. D., MacNicol, D. D., Vögtle, F., Eds.; Pergamon: New York, 1996; Chapter 9. (d) Piotrowiak, P. *Chem. Soc. Rev.* **1999**, *28*, 143–150. (e) Wasielewski, M. R. *Acc. Chem. Res.* **2009**, *42*, 1910–1921.
(17) (a) Sessler, J. L.; Wang, B.; Harriman, A. *J. Am. Chem. Soc.* **1993**, *115*, 10418–10419. (b) de Rege, P. J. F.; Williams, S. A.; Therien, M. J. *Science* **1995**, *269*, 1409–1413. (c) Rosenthal, J.; Hodgkiss, J. M.; Young, E. R.; Nocera, D. G. *J. Am. Chem. Soc.* **2006**, *128*, 10474–10483. (d) D'Souza, F.; Gadde, S.; Islam, D.-M. S.; Pang, S.-C.; Schumacher, A. L.; Zandler, M. E.; Horie, R.; Araki, Y.; Ito, O. *Chem. Commun.* **2007**, 480–482. (e) Gadde, S.; Islam, D.-M. S.; Wijesinghe, C. A.; Subbaiyan, N. K.; Zandler, M. E.; Araki, Y.; Ito, O.; D'Souza, F. *J. Phys. Chem. C* **2007**, *111*, 12500–12503. (f) Wessendorf, F.; Gnichwitz, J.-F.; Sarova, G. H.; Hager, K.; Hartnagel, U.; Guldi, D. M.; Hirsch, A. *J. Am. Chem. Soc.* **2007**, *129*, 16057–16071. (g) Gnichwitz, J.-F.; Wielopolski, M.; Hartnagel, K.; Hartnagel, U.; Guldi, D. M.; Hirsch, A. *J. Am. Chem. Soc.* **2008**, *130*, 8491–8501. (h) D'Souza, F.; Venukadasula, G. M.; Yamanaka, K.-I.; Subbaiyan, N. K.; Zandler, M. E.; Ito, O. *Org. Biomol. Chem.* **2009**, *7*, 1076–1080.
(18) (a) Guldi, D. M.; Fukuzumi, S. *J. Porphyrins Phthalocyanines* **2002**, *6*, 289–295. (b) Guldi, D. M. *Pure Appl. Chem.* **2003**, *75*, 1069–1075.
(19) (a) Sanchez, L.; Martin, N.; Guldi, D. M. *Angew. Chem.* **2005**, *117*, 5508–5516; *Angew. Chem., Int. Ed.* **2005**, *44*, 5374−5382. (b) Sanchez, L.; Sierra, M.; Martin, N.; Myles, A. J.; Dale, T. J.; Rebek, J., Jr.; Seitz, W.; Guldi, D. M. *Angew. Chem.* **2006**, *118*, 4753–4757; *Angew. Chem., Int. Ed.* **2006**, *45*, 4637−4641. (c) Sandanayaka, A. S. D.; Araki, Y.; Ito, O.; Chitta, R.; Gadde, S.; D'Souza, F. *Chem. Commun.* **2006**, 4327–4329. (d) D'Souza, F.; Chitta, R.; Gadde, S.; Zandler, M. E.; Sandanayaka, A. S. D; Araki, Y.; Ito, O. *Chem. Commun.* **2005**, 1279–1281. (e) D'Souza, F.; Chitta, R.; Gadde, S.; McCarty, A. L.; Karr, P. A.; Zandler, M. E.; Sandanayaka, A. S. D.; Araki, Y.; Ito, O. *J. Phys. Chem. B* **2006**, *110*, 5905–5913. (f) D'Souza, F.; El-Khouly, M. E.; Gadde, S.; Zandler, M. E.; McCarty, A. L.; Araki, Y.; Ito, O. *Tetrahedron* **2006**, *62*, 1967–1978. (g) D'Souza, F.; Chitta, R.; Gadde, S.; Rogers, L. M.; Karr, P. A.; Zandler, M. E.; Sandanayaka, A. S. D.; Araki, Y.; Ito, O. *Chem.-Eur. J.* **2007**, *13*, 916–922.
(20) (a) Chang, S.-K.; Hamilton, A. D. *J. Am. Chem. Soc.* **1988**, *110*, 1318–1319. (b) Hager, K.; Franz, A.; Hirsch, A. *Chem.-Eur. J.* **2006**, *12*, 2663–2679. (c) Hager, K.; Hartnagel, U.; Hirsch, A. *Eur. J. Org. Chem.* **2007**, *12*, 1942–1956. (d) Maurer, K.; Hager, K.; Hirsch, A. *Eur. J. Org. Chem.* **2006**, *15*, 3338–3347. (e) Franz, A.; Bauer, W.; Hirsch, A. *Angew. Chem.* **2005**, *117*, 1588–1561; *Angew. Chem., Int. Ed.* **2005**, *44*, 1564−1567.
(21) (a) Murakami, M.; Ohkubo, K.; Hasobe, T.; Sgobba, V.; Guldi, D. M.; Wessendorf, F.; Hirsch, A.; Fukuzumi, S. *J. Mater. Chem.* **2010**, *20*, 1457–1466. (b) Wessendorf, F.; Hirsch, A. *Tetrahedron* **2008**, *64*, 11480–11489.
(22) (a) Goldsmith, R. H.; Sinks, L. E.; Kelley, R. F.; Betzen, L. J.; Liu, W.; Weiss, E. A.; Ratner, M. A.; Wasielewski, M. R. *Proc. Natl. Acad. Sci. U.S.A.* **2005**, *102*, 3540–3545. (b) Weiss, E. A.; Tauber, M. J.; Kelley, R. F.; Ahrens, M. J.; Ratner, M. A.; Wasielewski, M. R. *J. Am. Chem. Soc.* **2005**, *127*, 11842–11850. (c) Tauber, M. J.; Kelley, R. F.; Giaimo, J. M.; Rybtchinski, B.; Wasielewski, M. R. *J. Am. Chem. Soc.* **2006**, *128*, 1782–1783. (d) Goldsmith, R. H.; Wasielewski, M. R.; Ratner, M. A. *J. Phys. Chem. A* **2006**, *110*, 20258–20262.

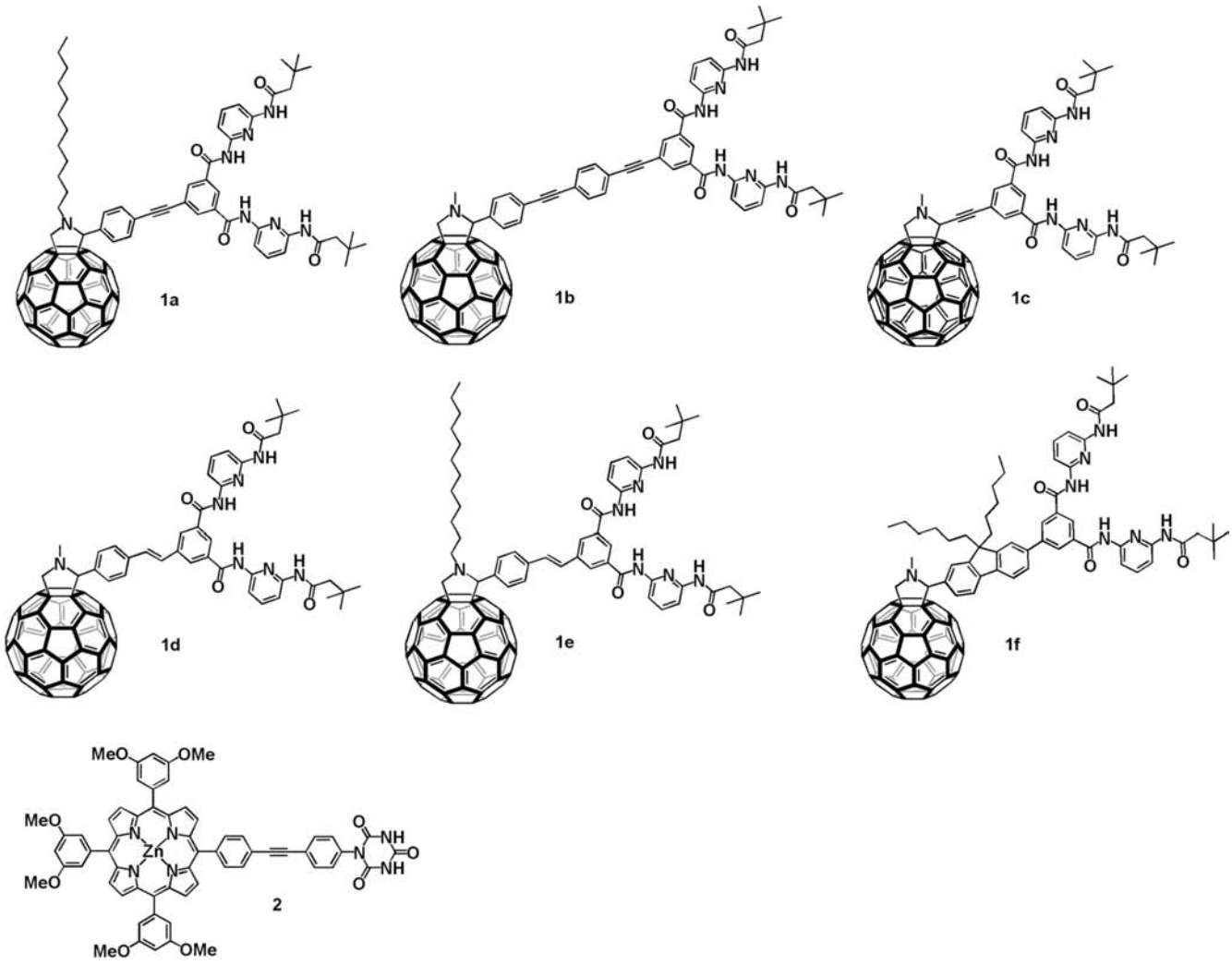

Figure 2. Synthesized fullerene **1** and porphyrin **2** derivatives.

Notable in the case of the aforementioned metalloporphyrin/fullerodendrimer assemblies with flexible alkyl chains, which were introduced as spacers, may have well been the inception to inter- and/or intramolecular folding. Conjugated spacers (i.e., *p*-phenylene-ethynylene, *p*-phenylene-vinylene, *p*-ethynylene, and fluorene), on one hand, provide wire-like behavior in terms of electron transfer/electron transport and, on the other hand, restrict the flexibility of the Hamilton receptor and cyanuric acid functionalities. The wire-like behavior is key to guaranteeing an efficient electronic coupling between the electroactive units if the following factors are provided: (i) matching the donor/acceptor and bridge energy levels, (ii) good electronic coupling between the donor and acceptor by means of the bridge orbitals,[20] and (iii) a small attenuation factor (β).[23] Intramolecular electron transfer/electron transport along π-conjugated oligomers, such as *o*-phenylenevinylene (oPV), has been tested in several donor−acceptor conjugates involving porphyrins,[24] anilins,[25] or ferrocenes[26] as electron donors and C_{60} as electron acceptor. In fact, recent studies have shown that the electron transfer along oPVs is much more efficient than that along *o*-fluorenes (oFl) or *o*-phenylene-ethynylenes (oPE). Such a trend is caused by a complete delocalization of π-electrons in oPVs, whereas the electron delocalization in oPE resides mostly on the phenyl rings. The electron delocalization in oFls can be found between both extremes.[27]

Here, we report on the study of electron transfer along π-conjugated spacers in a novel series of supramolecular assembled porphyrin/fullerene hybrids. In light of the aforementioned, we have integrated *p*-phenylene-ethynylene, *p*-phenylene-vinylene, *p*-ethynylene, or fluorene units as spacers between fullerenes and the Hamilton receptors as well as a *p*-phenylene-ethynylene bridged porphyrinato cyanuric acid (Figure 2) and have analyzed the attenuation factor (β).

(23) (a) Muellen, K.; Wegner, G. *Electronic Materials: The Oligomer Approach*; Wiley-VCH: Weinheim, Germany, 1998. (b) Atienza-Castellanos, C.; Wielopolski, M.; Guldi, D. M.; van der Pol, C.; Bryce, M. R.; Filippone, S.; Martin, N. *Chem. Commun.* **2007**, 5146–5166.

(24) (a) Redmore, N. P.; Rubstov, I. V.; Therien, M. J. *J. Am. Chem. Soc.* **2003**, *125*, 8769–8778. (b) Screen, T. O.; Thorne, J. R. G.; Denning, R. G.; Bucknall, D. G.; Anderson, H. L. *J. Mater. Chem.* **2003**, *13*, 2796–2808.

Scheme 1. Syntheses of Hamilton Receptor Bearing **4** and **8**[a]

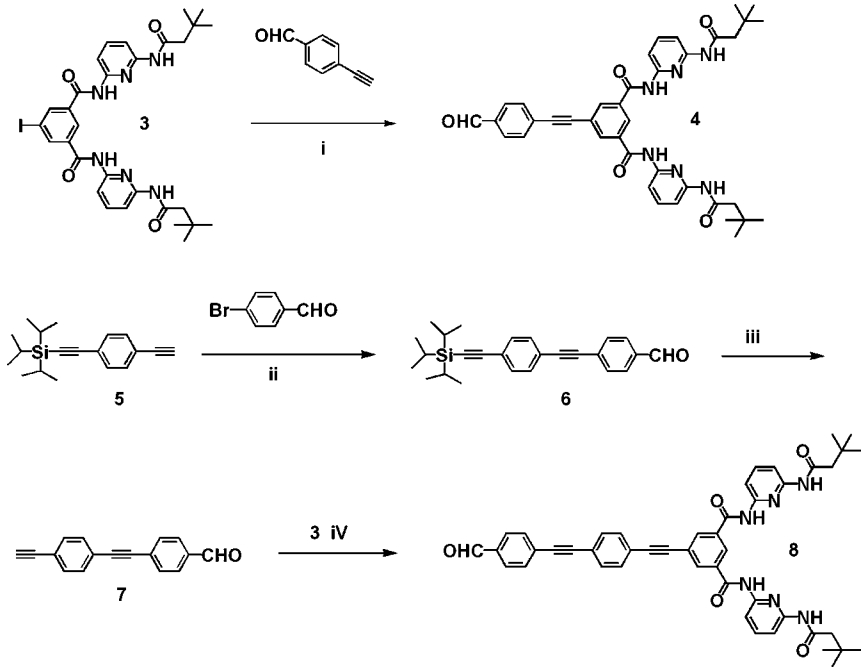

[a] (i) $Pd(PPh_3)_2Cl_2$, CuI, NEt_3, THF, room temperature; (ii) $Pd(PPh_3)_2Cl_2$, CuI, $HNEt_2$, toluene, 75 °C; (iii) TBAF, THF, 0 °C; (iv) $Pd(PPh_3)_2Cl_2$, CuI, NEt_3, THF, room temperature.

Results

Synthesis. From the synthetic point of view, iodo compound[21b] **3** (Scheme 1) is the key compound en-route toward **1**. Subsequent C−C cross coupling reactions were performed under Sonogashira conditions involving terminal alkynes and aryl halides.[28]

The need for further functionalization of the Hamilton receptor via, for example, the Prato reaction of C_{60}[29] required the implementation of formyl groups in para position relative to the cross-coupled aryl groups. To combine both synthetic necessities, 4-ethynylbenzaldehyde was used as a promising reagent toward iodo compound **3**. The coupling of both compounds was nearly quantitative at room temperature[21a] (Scheme 1).

Extension of the *p*-phenylene-ethynylene chain was performed by using 4-bromobenzaldehyde and (2-(4-ethynylphenyl)ethynyl)triisopropylsilane **5**, which were coupled using Pd^0/Cu^I catalysis at 75 °C (Scheme 1). Deprotecting the resulting *p*-phenylene-ethynylene using TBAF (tetrabutyl ammonium fluoride) as fluoride source led to the terminal ethynyl derivative **7**. The latter was subsequently coupled to the Hamilton receptor building block, as described above for 4-ethynyl benzaldehyde, to afford **8** (Scheme 1). To investigate the influence of the bridge's nature on the photophysical properties, Hamilton receptor bearing fullerenes that are not only connected by *p*-phenylene-ethynylene chains **1a**,**b**, but also by *p*-ethynylene **1c**, *p*-phenylene-vinylene **1d**,**e** and fluorene **1f** spacers, were designed. The *p*-ethynyl precursor **9** was accessible by reacting 3,3-diethoxyprop-1-yne with iodo Hamilton receptor **3** under Pd^0/Cu^I catalysis in tetrahydrofurane and diethylamine. Deprotection of the acetal by adding TFA (trifluoro acetic acid) and subsequent neutralization with sodium bicarbonate afforded the ethynyl Hamilton receptor **10**, Scheme 2.

To introduce a *p*-phenylene-vinylene spacer, we synthesized 4-ethenyl benzaldehyde **11** by adding *n*-BuLi and DMF to 4-bromostyrene at −78 °C. Heck conditions were then applied for coupling 4-ethenylbenzaldehyde and iodo Hamilton receptor **3** to give the *p*-phenylene-vinylene Hamilton receptor **12** using Pd_2dba_3 (tris(dibenzylideneacetone)dipalladium(0)) as Pd^0 source and triphenyl arsine as additional ligand, Scheme 2.[30] The fluorene containing precursor **14** was obtained by Suzuki coupling of boronic acid ester **13** and Hamilton receptor **3** under the action of $Pd(PPh_3)_4$ and potassium carbonate (Scheme 2).[31] To increase the solubility of the *p*-phenylene-ethynylene and *p*-phenylene-vinylene containing fullerene derivatives in common organic solvents, we synthesized *N*-dodecyl glycine **15** by adding iodo acetic acid to dodecylamine at 0 °C in a mixture of ethanol and water (Scheme 3).[32]

The wire-like Hamilton receptor fullerenes **1** were then synthesized following the standard Prato protocol, that is, allowing C_{60} to react with aldehydes **4**, **8**, **10**, **12**, **14**, and sarcosine or *N*-dodecyl glycine **15** in THF/toluene under reflux (Scheme 4).[29]

(25) (a) Thomas, K. G.; Biju, V.; Guldi, D. M.; Kamat, P. V.; George, M. V. *J. Phys. Chem. B* **1999**, *103*, 8864–8869. (b) Guldi, D. M.; Swartz, A.; Luo, C.; Gomez, R.; Segura, J. L.; Martin, N. *J. Am. Chem. Soc.* **2002**, *124*, 10875–10886.
(26) Dong, T.-Y.; Chang, S.-W.; Kin, S.-F.; Lin, M.-C.; Wen, Y.-S.; Lee, L. *Organometallics* **2006**, *25*, 2018–2024.
(27) Wielopolski, M.; Atienza, C.; Clark, T.; Guldi, D. M.; Martin, N. *Chem.-Eur. J.* **2008**, *14*, 6379–6390.
(28) (a) Nagy, A.; Novak, Z.; Kotschy, A. *J. Organomet. Chem.* **2005**, *69*, 4453–4461. (b) Tykwinski, R. R. *Angew. Chem., Int. Ed.* **2003**, *42*, 1566–1568.
(29) Maggini, M.; Scorrano, G.; Prato, M. *J. Am. Chem. Soc.* **1993**, *115*, 9798–9799.
(30) Stewart, J. J. P. *J. Comput. Chem.* **1989**, *209*, 221–264.
(31) Heck, R. F.; Nolley, J. P., Jr. *J. Org. Chem.* **1972**, *37*, 2320–2322.
(32) (a) Miyaura, N.; Yamada, K.; Suzuki, A. *Tetrahedron Lett.* **1979**, *36*, 3437–3440. (b) Suzuki, A. *J. Organomet. Chem.* **1999**, *576*, 147–168.

Scheme 2. Syntheses of Hamilton Receptor Bearing **10**, **12**, and **14**[a]

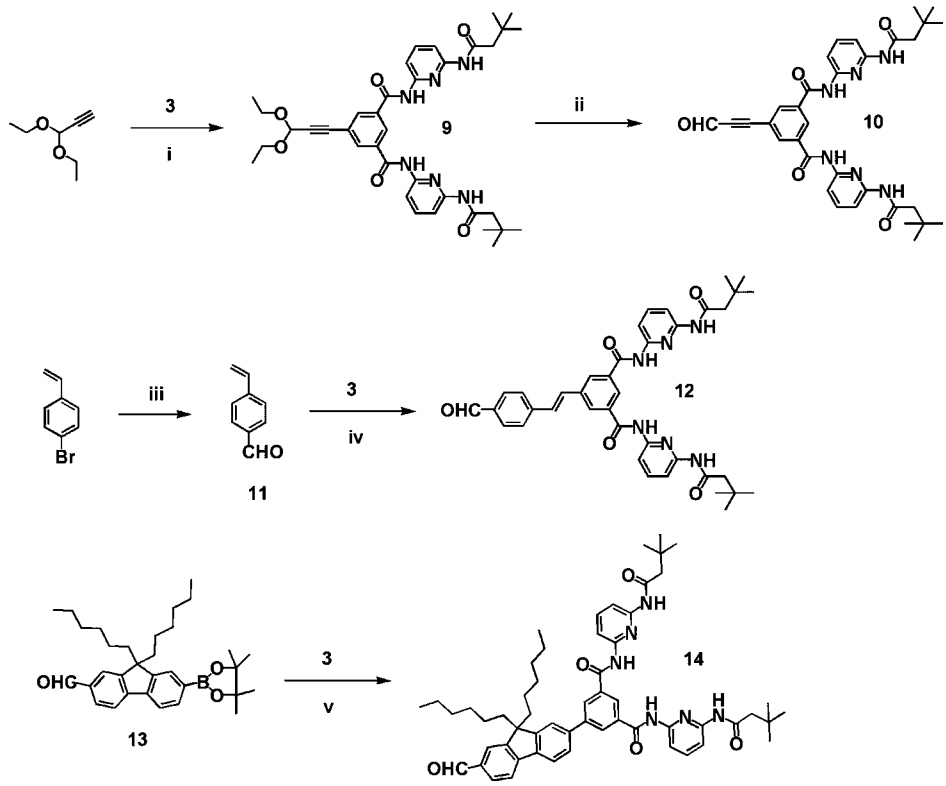

[a] (i) $Pd(PPh_3)_2Cl_2$, CuI, $HNEt_2$, THF, room temperature; (ii) (1) TFA, CH_2Cl_2, room temperature, (2) $H_2O/NaHCO_3$, room temperature; (iii) (1) *n*-BuLi, THF, −78 °C, (2) DMF, −78 °C, (3) H_2O/NH_4Cl, room temperature; (iv) Pd_2dba_3, $AsPh_3$, NEt_3, THF, 70 °C; (v) $Pd(PPh_3)_4$, K_2CO_3, DMF, room temperature.

Scheme 3. Synthesis of *N*-Dodecyl Glycine **15**[a]

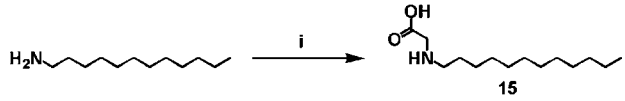

[a] (i) Iodo acetic acid, $EtOH/H_2O$, 0 °C.

The cyanuric acid bearing porphyrin **2**, on the other hand, was synthesized in accordance with our recently published procedure.[21b]

Molecular Modeling. To determine the length of the π-conjugated spacers (i.e., *p*-phenylene-ethynylene, *p*-phenylene-vinylene, *p*-ethynylene, and fluorene) as part of the Hamilton receptor carrying fullerenes, we carried out molecular mechanics calculations. In addition, it assists in shedding light onto their rigidity as an important means to guarantee efficient electron transfer along the π-conjugated spacers and to eliminate through-space electron transfer fostered by inter- or intramolecular folding. All calculations, PM3 geometry optimization in the gas phase,[30] revealed rigid geometries, regardless of the conjugated spacer type. In terms of spacer lengths, varying distances were obtained for *p*-phenylene-vinylene, *p*-ethynylene, and fluorene-based Hamilton receptor fullerenes. Moreover, introduction of an additional *p*-phenylene-ethynylene unit goes in hand with an increase in distance from 12.2 to 19.1 Å; see Figure 3 and Table 1.

NMR-Titration Experiments. Initial insight into the formation of the **1·2** complexes was lent from ^1H NMR spectroscopy.

Scheme 4. Syntheses of the Hamilton Receptor Bearing Fullerene Derivatives **1**[a]

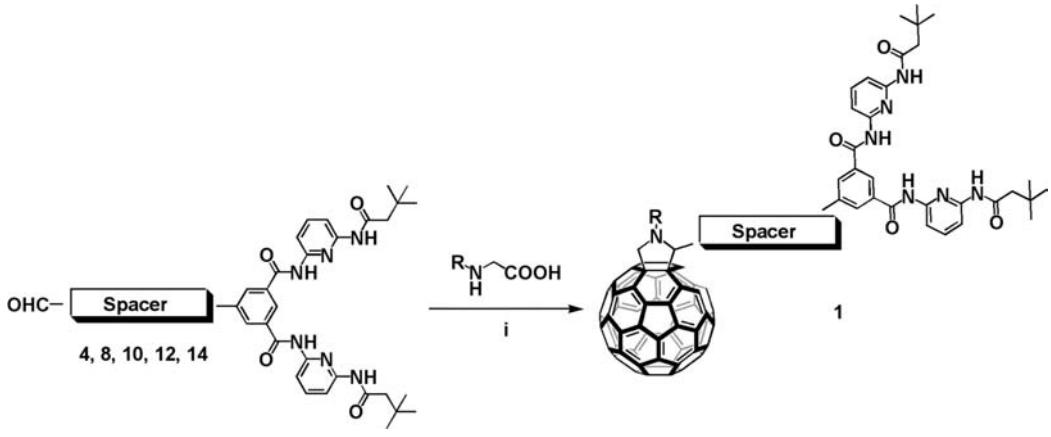

[a] (i) C_{60}, toluene, reflux.

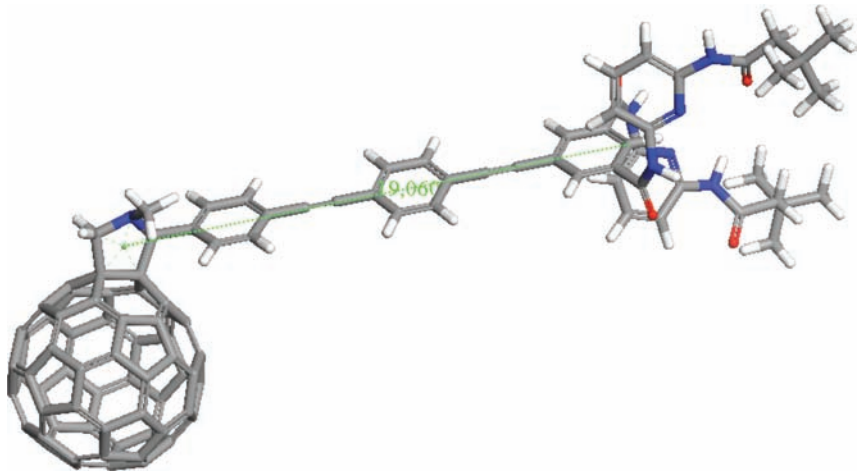

Figure 3. PM3-optimized structure of **1b**.

Table 1. Spacer Distance, Association Constants K_{ass}, Absorption Decrease, Fluorescence Quenching Efficiency, Charge Separation, and Charge Recombination Dynamics, Determined via Femtosecond and Nanosecond Transient Absorption Measurements

			log K_{ass}[c]				rate constants[d]	
	spacer distance,[a] Å	log K_{ass},[b] $CDCl_3$	oDCB	CH_2Cl_2	absorption decrease, %	quenching efficiency, %	k_{CS}, s^{-1}	k_{CR}, s^{-1}
1a·2	12.2	5.318 ± 1.11	3.528 ± 0.3	3.719 ± 0.4	13	17	3.1×10^9	1.4×10^7
1b·2	19.1		2.182 ± 0.5	2.698 ± 0.7	not observed	4	not detectable	not detectable
1c·2	7.9			4.667	24	30	1.1×10^{10}	3.3×10^7
1d·2	12.0	5.175 ± 1.05	4.089 ± 0.4	4.332 ± 0.4	16	25	5.3×10^9	2.5×10^7
1f·2	13.8	5.163 ± 1.09	4.104 ± 0.4	4.201 ± 0.4	9	22	4.1×10^9	1.9×10^7

[a] See Molecular Modeling section. [b] Obtained from ^{1}H NMR titration experiments. [c] Obtained from fluorescence titration experiments. [d] Rate constants for charge separation (k_{CS}) and charge recombination (k_{CR}) were calculated from the transient absorption data.

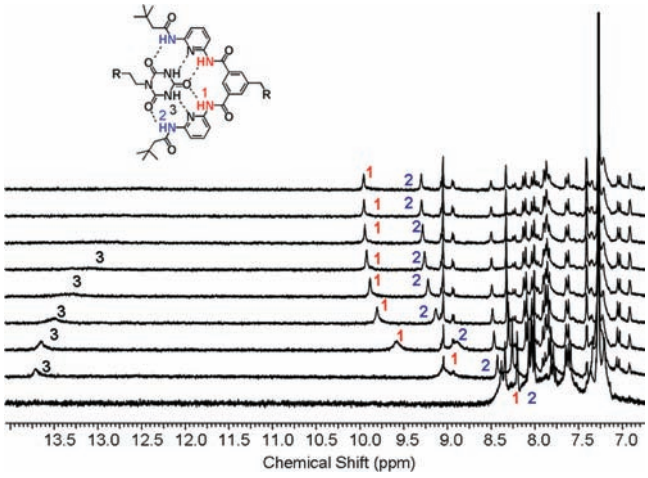

Figure 4. Binding motif between **1a**,**e**,**f** and **2** with indication of the NH protons NH1, NH2, and NH3 (top) and 300 MHz ^{1}H NMR spectra of **1a** at a concentration of 3.3 mM in $CDCl_3$ in the presence of various equivalents of **2** (bottom).

Here, the determination of the association constant K_{ass} was achieved through a complementary series of titration experiments in $CDCl_3$. In particular, the characteristic downfield shifts of the NH^1- and NH^2-protons of the Hamilton-receptor moieties in **1** emerged as suitable markers for the complex formation.[17a,20,21] In Figure 3, the corresponding shifts of the protons of **1** are depicted as they change as a function of added fullerene **2**. Additionally, the shifts of the NH^3-protons within the cyanuric acid moiety of **2** were investigated (Figure 4). In a typical experiment, 500 μL of a 2 mM solution of **1a**, **1e**, **1f** was titrated with 100 μL of a 2 mM solution of porphyrin **2**. The ^{1}H NMR spectra were recorded approximately 30 min after mixing the solutions. In each case, the spectrum remained unchanged during a time period of 60 min, indicating a fast equilibrium.

Whereas the NH^1- and NH^2-protons undergo a shift to lower fields, the NH^3-protons of the cyanuric acid moieties at 13 ppm are subject to an opposite effect. The corresponding signals undergo a high field shift during addition of **2**. Furthermore, they broaden, and, finally, they disappear. The reason for the disappearance in the presence of an excess of **2** is a fast equilibrium (coalescence regime) between bound and free cyanurate. On the basis of these titration experiments, the association constants K_{ass} (Table 1) were determined with the help of Chem-Equili.[33]

A plot of the chemical shift (δ [ppm]) of the NH protons as a function of mole fraction X of titrated cyanuric acid bearing porphyrin **2** reveals the characteristic sigmoidal shape with a plateau at $X = 1$; see Figure 5. We take the latter as preliminary evidence for the **1·2** formation with a 1:1 stoichiometry.

Photophysical Characterization. Further information on the supramolecular complexation was obtained by optical absorption spectroscopy and steady-state fluorescence spectroscopy. To this end, variable amounts of the different Hamilton receptors (i.e., **1a**, **1b**, **1c**, **1d**, **1e**, or **1f**) were added to porphyrinato cyanuric acid (**2**) containing *ortho*-dichlorobenenzene or dichloromethane solutions. Importantly, upon increasing gradually the concentration of **1a**, **1b**, **1c**, **1d**, **1e**, or **1f**, the Soret band of **2** is slightly decreased without, however, giving rise to any spectral shifts.[17c] Notable is, however, that the overlapping absorptions of **1a**, **1b**, **1c**, **1d**, **1e**, or **1f** and **2** prevent the formation of clear isosbestic points in the 415 and 429 nm range.

(33) (a) Solov'ev, V. P.; Vnuk, E. A.; Strakhova, N. N.; Reavsky, O. A. *VINITI*; Moscow, 1991. (b) Solov'ev, V. P.; Baulin, V. E.; Strahova, N. N.; Kazachenko, V. P.; Belsky, V. K.; Varnek, A. A.; Volkova, T. A.; Wipff, G. *J. Chem. Soc., Perkin Trans. 1* **1998**, 1489–1498.

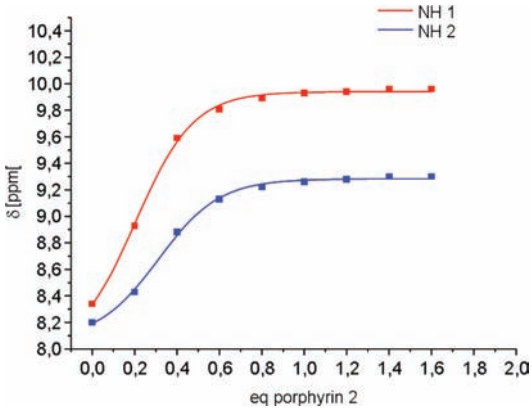

Figure 5. Plot of the chemical shift (δ [ppm]) of the NH1 and NH2 as a function of mole fraction X of titrated cyanuric acid bearing porphyrin **2**.

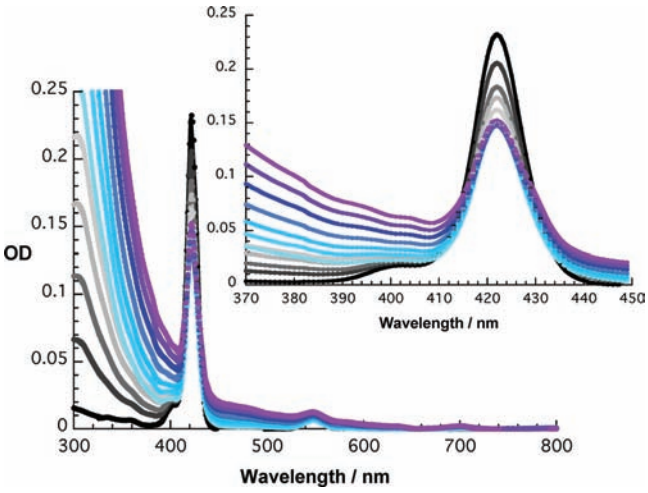

Figure 6. Changes in the Zn porphyrin **2** (2.83×10^{-6} M) electronic absorption spectrum in CH_2Cl_2 upon addition of increasing concentrations of C_{60} derivative **1d** ($0-1.0 \times 10^{-5}$ M) at room temperature.

It is interesting to note that the strength of the spectral changes seems to relate to the nature of the spacer (Figure 6). For **1a·2**, **1d·2**, **1e·2**, and **1f·2**, the spectral changes, as they evolve during the titration, are rather marginal, whereas noticeable alterations emerge for **1c·2**. Opposing to the aforementioned trend, titrating **2** with **1b** resulted in what is best described as the simple superimposition of the individual spectra; see the Supporting Information. In general, our current observations, detectable but rather weak spectroscopic changes, are in stark contrast to previous studies.[17a] A likely rationale implies that introducing rigid spacers constrains the ground-state interactions between **1** and **2**.

To gain quantitative details on the binding strength, complementary fluorescence titration experiments were carried out. In line with earlier work, the prominent fluorescence of **2** ($\Phi_F = 0.04$) was monitored while variable amounts of **1a**−**d** were added. Figure 7 illustrates an exemplary case, in which **2** was titrated with **1d** in dichloromethane. The gradual quenching at the long wavelength maximum of the emission was used to estimate the association constant according to eq 1:

$$\frac{I_f}{I_0} = 1 - \frac{1}{2c_D}\left[\frac{1}{K_s} + c_0 + c_D - \sqrt{\left(\frac{1}{K_s} + c_0 + c_D\right)^2 - 4c_0c_D}\right] \quad (1)$$

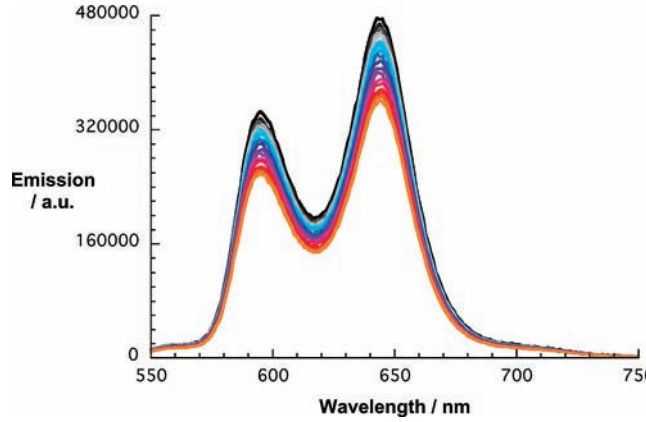

Figure 7. Steady-state fluorescence spectra of **2** (2.3×10^{-6} M) recorded at different concentrations of **1d** ($0-2.10 \times 10^{-5}$ M) in CH_2Cl_2 at room temperature ($\lambda_{exc} = 416$ nm).

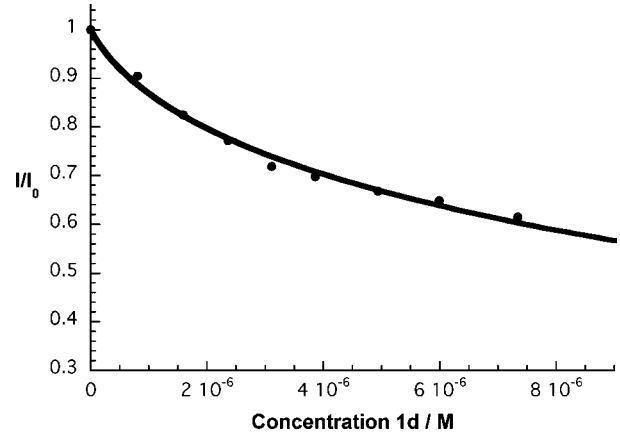

Figure 8. Plot of I/I_0 versus concentration of **1d** used to determine the association constant (according to eq 1).

Here, I_o refers to the initial fluorescence intensity, c_o is the total porphyrin concentration, c_D is the total concentration of the added fullerene, and K_{ass} is the association constant (Figure 8).[34]

The association constants deduced from the fluorescence experiments are listed in Table 1. Considering the error margins, which are 10% in the case of **1a**, **1d**, **1e**, and **1f** and 25% in the case of **1b**, a reasonably good agreement is achieved with the association constants based on the ^{1}H NMR experiments.

Next, we turned to time-resolved fluorescence. To this end, porphyrinato cyanuric acid **2** was excited at 403 nm at different ratios with **1a**, **1b**, **1c**, **1d**, **1e**, or **1f**, and the resulting fluorescence time profiles were analyzed by mono-, bi-, or even poly exponential decay fitting functions. In the absence of **1a**, **1b**, **1c**, **1d**, **1e**, or **1f**, the fluorescence decay of **2** was strictly fitted by a monoexponential fitting function that yielded lifetimes of about 1.5 ns in *ortho*-dichlorobenzene as well as in chloroform. Addition of **1a**, **1b**, **1c**, **1d**, **1e**, or **1f** led to the following consequence. Now, a satisfying fit of the fluorescence time profiles is only achieved when a biexponential fitting function is employed. Besides the 1.5 ns lifetime, a shorter lifetime in the range of hundreds of picoseconds emerges. While the earlier is clearly associated with the intrinsic decay of **2**, the latter reflects the accelerated excited-state deactivation in successfully formed **1·2**. Interestingly, no appreciable changes resulted in the presence of **1b**, just the 1.5 ns lived component.

(34) Valeur, B. *Molecular Fluorescence*; Wiley-VCH: Weinheim, 2002.

In complementary experiments, we varied the concentration of **1a**, **1b**, **1c**, **1d**, **1e**, or **1f** incrementally. Here, analyses of the pre-exponential factors of both lifetimes demonstrated that an increase of **1a**, **1b**, **1c**, **1d**, **1e**, or **1f** causes an increase of the pre-exponential factor of the short-lived contributions and, simultaneously, a decrease of the pre-exponential factor of the long-lived component. Importantly, the absolute values of the short- and the long-lived components remained unchanged throughout these assays.

Results from the steady-state and time-resolved experiments prompt one to a fairly fast and efficient deactivation of photoexcited **1·2**, presumably via electron transfer to the electron-accepting fullerene, while energy transfer cannot be ruled out. Notable is in this context that excited-state contributions (i.e., singlet and triplet excited states) as they originate from an inefficient fluorescence quenching in **1·2** and/or incomplete association of **1·2** render the quantification of a transduction of excited-state energy intrinsically difficult. Thus, femtosecond transient absorption spectroscopic measurements were performed to unveil the deactivation process and, in addition, to analyze its kinetics. The differential absorption changes, taken right after 150 fs laser pulse excitation of **2** at 420 nm in *ortho*-dichlorobenzene, show in the absence of any **1a**, **1b**, **1c**, **1d**, **1e**, or **1f** the prompt transformation (i.e., 5.6×10^8 s^{-1}) of the high lying singlet excited states of the porphyrin into the lowest vibrational state of the porphyrin singlet excited state.[35,36] In particular, marked transitions develop in the region between 600 and 1100 nm. Besides these characteristics, bleach features as they relate to the ground-state absorptions are found around 420 nm as well as at 550 and 600 nm. This singlet excited state with an energy of about 2.00 eV deactivates slowly via intersystem crossing to the energetically lower lying triplet excited state, which is located at around 1.53 eV.[37] The rate constant of intersystem crossing was determined from a multiwavelength analysis to be 4.6×10^8 s^{-1}. The newly developing band at 840 nm reflects the diagnostic signature of the triplet excited state of **2** with a lifetime of 45 μs. In the presence of molecular oxygen, the triplet excited state experiences a concentration-dependent deactivation process to form singlet oxygen quantitatively.[36]

Upon excitation of **1a**, **1b**, **1c**, **1d**, **1e**, or **1f** at 387 nm, the lowest vibrational state of the initially generated singlet excited state undergoes quantitative intersystem crossing with a rate constant of 5×10^8 s^{-1} to the energetically lower lying long-lived triplet excited state. Characteristic absorptions of the singlet excited state are seen at 510 and 920, while maxima at 360 and 720 nm and a low-energy shoulder around 800 nm are associated with the triplet features.[9,37,38] In the absence of molecular oxygen, the triplet excited states of **1a**, **1b**, **1c**, **1d**, **1e**, or **1f** have a lifetime of up to 20 μs.

The presence of **1a**, **1c**, **1d**, **1e**, or **1f** impacts the reactivity of the cyanuric bearing porphyrin **2**. Because of the strong and dominant absorption of **2** in **1a·2**, **1c·2**, **1d·2**, **1e·2**, and **1f·2**, visible light excitation at 420 or 550 nm is expected to lead predominantly to the formation of the porphyrin singlet excited state; see Figure S2 for the transient absorption spectrum of **2**. This is confirmed by transient features such as transient bleaching at 420, 550, and 600 nm and transient absorption from 570 to 750 nm. However, this species undergoes a fast decay in sharp contrast to the slow decay of **2** to generate the triplet excited state. Concomitant with the singlet excited-state decay of **2** in the 400−800 nm range, new features appeared in the 800−1200 nm range. In particular, a maximum at 1000 nm is a reliable attribute of the one-electron reduced form of fullerenes, indicating that deactivation of the singlet excited state of **2** occurs by electron transfer.[39] Evidence for the one-electron oxidized porphyrins was found in the 600−800 nm range, where its diagnostic absorption developed in parallel; see Figure 9.[40] A multiwavelength analysis led to a major decay component with a lifetime of 326 ps, which we attributed to charge separation affording the radical ion pair state. The rates of charge separation were derived for all systems and are listed in Table 1. Importantly, the radical ion pair species is stable on the 3 ns time scale of our femtosecond experiments.

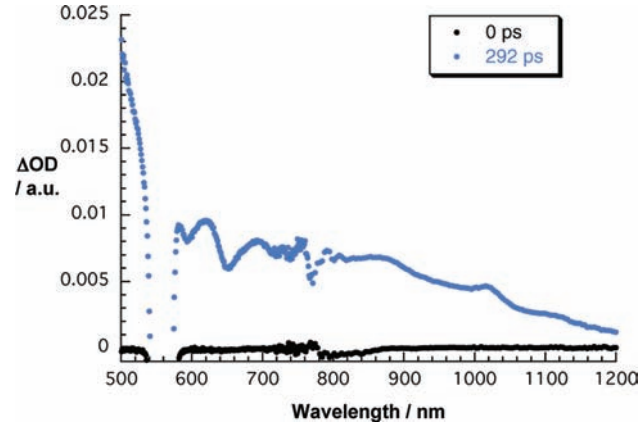

Figure 9. Differential absorption spectra (visible and near-infrared) obtained upon femtosecond flash photolysis (550 nm) of **1a·2** in argon-saturated *ortho*-dichlorobenzene with time delays of 0 and 292 ps at room temperature.

Interestingly, introduction of a second *p*-phenylene-ethynylene repeat unit (i.e., **1a·2** versus **1b·2**) eliminates the electron transfer process with no evidence for any radical ion pair state formation, Figure 10. This finding is well in line with our steady-state and time-resolved fluorescence measurements. In fact, it supports the notion that in photoexcited **1b·2**, intrinsic deactivation pathways, as for example, fluorescence and intersystem crossing, dominate rather than electron transfer that has been seen to be the case in **1a·2**.

In the final part, nanosecond transient absorption measurements were employed to follow the charge recombination processes in **1·2** upon 6 ns lasting 532 nm excitation in argon-saturated *ortho*-dichlorobenzene solutions. The product of charge separation, that is, the one-electron oxidized porphyrin and the one-electron reduced fullerene, was partly masked by the strong excited-state features of free, uncomplexed **2**, **1a**, **1c**, **1d**, **1e**, and **1f**. These emerge in the 580−900 nm range despite the

(35) (a) Hoffman, M. Z.; Bolletta, F.; Moggi, L.; Hug, G. L. *J. Phys. Chem. Ref. Data* **1989**, *18*, 219–543. (b) Rodriguez, J.; Kirmaier, C.; Holten, D. *J. Am. Chem. Soc.* **1989**, *111*, 6500–6509. (c) Murov, S. L.; Carmichael, I.; Hug, G. L. *Handbook of Photochemistry*; Marcel Dekker Inc.: New York, 1993;

(36) Kalyanasundaram, K. *Photochemistry of Polypyridine and Porphyrin Complexes*; Academic Press: London, 1992.

(37) Luo, C.; Guldi, D. M.; Imahori, H.; Tamaki, K.; Sakata, Y. *J. Am. Chem. Soc.* **2000**, *122*, 6535–6551.

(38) Nojiri, T.; Watanabe, A.; Ito, O. *J. Phys. Chem. A* **1998**, *102*, 5215–5219.

(39) (a) Guldi, D. M.; Hungerbuehler, H.; Janata, E.; Asmus, K. D. *J. Chem. Soc., Chem. Commun.* **1993**, *6*, 84–86. (b) Kato, T.; Kodama, T.; Shida, T.; Nakagawa, T.; Matsui, Y.; Suzuki, S.; Shiromaru, H.; Yamauchi, K.; Achiba, Y. *Chem. Phys. Lett.* **1991**, *180*, 446–450.

(40) Guldi, D. M.; Hirsch, A.; Scheloske, M.; Dietel, E.; Troisi, A.; Zerbetto, F.; Prato, M. *Chem.-Eur. J.* **2003**, *9*, 4968–4979.

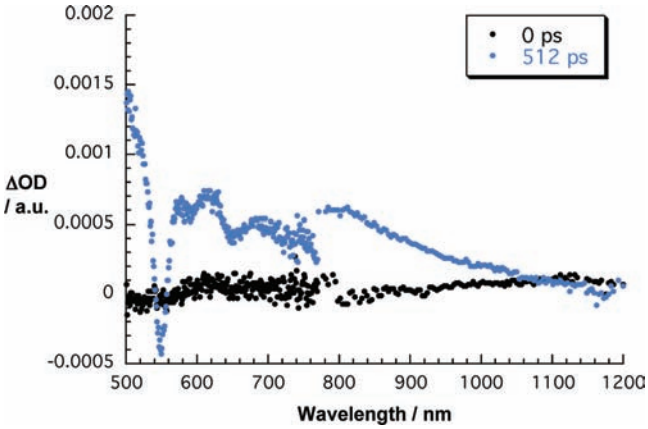

Figure 10. Differential absorption spectra (visible and near-infrared) obtained upon femtosecond flash photolysis (420 nm) of **1b·2** in argon-saturated *ortho*-dichlorobenzene with time delays of 0 and 512 ps at room temperature.

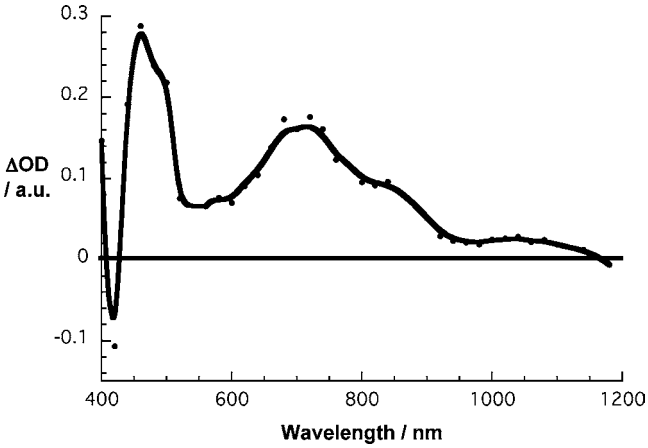

Figure 11. Differential absorption spectra (visible and near-infrared) obtained upon nanosecond flash photolysis (532 nm) of **1c·2** in Ar-saturated *ortho*-dichlorobenzene with a time delay of 80 ns.

rather high association constants of 10^3-10^4 M^{-1}, derived from the fluorescence assays, and 10^5 M^{-1}, derived from ^{1}H NMR experiments. Only around 1000 nm is the one-electron reduced fullerene seen with ease for **1a·2**, **1c·2**, **1d·2**, and **1f·2**. This led us to perform the same experiments but in the presence of molecular oxygen. Through the triplet deactivation of **1** and **2** to form singlet oxygen, the diagnostic features of the one-electron oxidized porphyrin came to light; see Figure 11.

Multiwavelength analyses of the transient absorption spectra in the absence of the triplet quenching oxygen gave rise to a biexponential decay behavior. On one hand, it is the lifetime of the triplet excited states of **1** (ca. 20 μs) and/or **2** (ca. 45 μs) and, on the other hand, a short lifetime that is on the order of several tens of nanoseconds. By purging the solutions with molecular oxygen, the triplet excited-state lifetimes of **1** and **2** were shortened from microseconds to hundreds of nanoseconds, without, however, affecting the short-lived component. Taking the aforementioned into consideration, we assign the second component to the charge recombination process. Please note that the accordingly determined rate constants for **1a·2**, **1c·2**, **1d·2**, and **1f·2** are listed in Table 1.

Finally, we calculated the β factor by plotting the rate constants of charge separation and charge recombination versus donor−acceptor distances; see Figure S3. Linear dependences

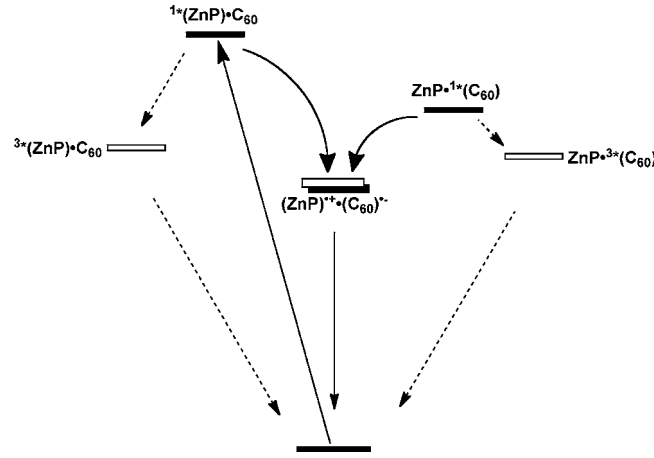

Figure 12. Energy diagram showing the deactivation pathways in **1·2**.

were observed in both cases, and the corresponding slopes were used to derive a β factor of 0.11 Å^{-1}. Notable is, however, that the determination of β infers spacers with different electron transfer activities. Still, this approximation sheds first light on supramolecular-based molecular wire systems with a β factor that lies between the extremes of covalent *p*-phenylene-ethynylene[27] and fluorene[23b] systems.

Discussion

This work sheds comprehensively and newly light onto a novel set of Hamilton receptor fullerenes (**1a**−**f**) and a cyanuric acid linked porphyrin (**2**). In particular, we have investigated the synthesis, self-assembly, and photophysical properties of novel supramolecular wire-like donor−acceptor nanohybrids using π-conjugated spacers of defined geometry, *p*-phenylene-ethynylene, *p*-phenylene-vinylene, *p*-ethynylene, and fluorene. Importantly, the 6-fold hydrogen-bonding motif prevents rotational freedom/structural flexibility and, in turn, strengthens the rigid confinement of the electron donor−acceptor nanohybrids. The rigidity was verified and illustrated by PM3 Molecular Modeling calculations. Dodecyl or hexyl chains were used to ensure sufficient solubility in a variety of solvents.

The self-assembly of **2** and **1a**−**f** was probed by means of ^{1}H NMR and fluorescence assays. Because of the exceptional strength of the 6-fold hydrogen bonding, association constants evolve in ^{1}H NMR experiments that are on the order of 10^5 M^{-1}, at millimolar concentrations. When, however, the association constants were considered that were derived from the characteristic changes in the fluorescence intensity, values emerged that are on the order of 10^4 M^{-1} for *p*-phenylene-ethynylene, *p*-phenylene-vinylene, and *p*-ethynylene spacers, respectively, at micromolar concentrations. The only notable exception is **1b** with an association constant of 10^2 M^{-1} that lacks electron transfer activity and, thus, just reflects a lower limit.

The spacer dependence, that is, length and nature, was corroborated by means of time-resolved techniques. In terms of simple distance dependence, transient absorption measurements confirm that the charge separation rate constants are 3.1×10^9 and 1.1×10^{10} s^{-1} for **1a·2** and **1c·2**, respectively. Interestingly, for **1b·2** no electron transfer activity was found on the time scale of up 3000 ps, which suggests that incorporation of an extra *p*-phenylene-ethynylene shuts down the electron transfer in **1b**. On the other hand, the rate constants in **1a·2**,

1d·2, and **1f·2** increase with decreasing attenuation factor of the spacer. Clearly, a correlation to a spacer-mediated dependence is likely. In fact, previous work has shown that the attenuation factors of π-conjugated oligomers increase in the order *p*-phenylene-vinylene > fluorene > *p*-phenylene-ethynylene.[27] Notable is the agreement with the results from our fluorescence assays. In particular, the fastest electron transfer, 5.3×10^9 s^{-1}, was observed for **1d·2**, followed by 4.1×10^9 (**1f·2**) and 3.1×10^9 s^{-1} (**1a·2**). Again, the fluorene-based **1f·2** is a more efficient π-conjuaged spacer than the *p*-phenylene-ethynylene-based **1a·2**. Energy transfer certainly emerges as a feasible alternative to the electron transfer scenario. However, contributions from an inefficient fluorescence quenching and an incomplete association toward the generation of singlet and triplet excited states mask the spectroscopic interpretation.

An overall resembling trend is seen for the charge recombination processes. The following trends correlate either with the nature of the spacer or with the length of the spacer. To this end, in the *p*-phenylene-ethynylene-based systems, the values of 1.4×10^7 (**1a·2**) and 3.3×10^7 s^{-1} (**1c·2**) reflect the change in spacer length, 12.2 versus 7.9 Å. It is worth re-emphasizing the lack of electron transfer activity in **1b·2**. On the other hand, varying the spacer motif from *p*-phenylene-ethynylene, fluorene, to *p*-phenylene-vinylene (i.e., **1a·2**, **1f·2**, and **1d·2**) results in a steady increase in charge recombination rate constant from 1.4×10^7 to 1.9×10^7 and to 2.5×10^{-7} s^{-1}. Here, the rate of charge recombination is, again, mainly governed by the nature of the spacer and not by its length. At this point, it is fair to conclude that the charge separation and charge recombination kinetics as they reflect either the length or the β factor of the employed spacer help to rationalize the conclusion of the fluorescence assays. Overall, a notably small β factor of 0.11 $Å^{-1}$ was obtained upon considering all electron donor−acceptor nanohybrids.

Conclusion

In short, we have demonstrated unambiguously that the electronic communication in rigid electron donor−acceptor nanohybrids that are brought together by the Hamilton receptor/cyanuric acid motif is controlled by the nature of the conjugated spacer moieties. Selective photoexcitation of the porphryins (2.0 eV) triggers in most hybrids an electron transfer to yield the one-electron reduced fullerenes and the one-electron oxidized porphyrins (1.4 eV); see Figure 12. Any appreciable contributions from a competitive energy transfer to populate the fullerene singlet excited state (1.78 eV) are masked by intrinsic formations. Spacers with good electron transfer properties (i.e., small β values) facilitate electron transfer along the supramolecular bridge and, in addition, cause an increase in the apparent association constants.

Acknowledgment. We thank the Fonds der Chemischen Industrie (FCI), Deutsche Forschungsgemeinschaft (SFB 583, Redoxaktive Metallkomplexe - Reaktivitätssteuerung durch molekulare Architekturen, and Exzellenzcluster, EAM - Engineering of Advanced Materials), for financial support.

Supporting Information Available: Experimental details and figures. This material is available free of charge via the Internet at http://pubs.acs.org.

JA101937W